Bounding the Higgs Boson Width through Interferometry

Lance J. Dixon and Ye Li

SLAC National Accelerator Laboratory, Stanford University, Stanford, California 94309, USA

(Received 24 May 2013; published 13 September 2013)

We study the change in the diphoton-invariant-mass distribution for Higgs boson decays to two photons, due to interference between the Higgs resonance in gluon fusion and the continuum background amplitude for $gg \to \gamma\gamma$. Previously, the apparent Higgs mass was found to shift by around 100 MeV in the standard model in the leading-order approximation, which may potentially be experimentally observable. We compute the next-to-leading-order QCD corrections to the apparent mass shift, which reduce it by about 40%. The apparent mass shift may provide a way to measure, or at least bound, the Higgs boson width at the Large Hadron Collider through "interferometry." We investigate how the shift depends on the Higgs width, in a model that maintains constant Higgs boson signal yields. At Higgs widths above 30 MeV, the mass shift is over 200 MeV and increases with the square root of the width. The apparent mass shift could be measured by comparing with the ZZ^* channel, where the shift is much smaller. It might be possible to measure the shift more accurately by exploiting its strong dependence on the Higgs transverse momentum.

DOI: 10.1103/PhysRevLett.111.111802 PACS numbers: 14.80.Bn, 12.38.Bx, 14.80.Ec

Introduction.—Recently, experiments at the Large Hadron Collider (LHC) have discovered a new boson with a mass around 125 GeV [1,2], whose properties are roughly consistent with those predicted for the standard model (SM) Higgs boson. It is now crucial to determine its properties as accurately as possible. The Higgs boson is dominantly produced by gluon fusion through a top quark loop. Its decay to two photons $H \to \gamma\gamma$ provides a very clean signature for probing Higgs properties, including its mass. However, there is also a large continuum background to its detection in this channel. It is important to study how much the coherent interference between the Higgs signal and the background could affect distributions in diphoton observables, and possibly use it to constrain Higgs properties.

The interference of the Higgs boson with $gg \to \gamma\gamma$ was first studied for an intermediate Higgs mass boson [3]. For the experimentally relevant case of a light, narrow-width Higgs boson, it is fruitful to divide the interference contribution into two parts, proportional to the real and imaginary parts of the Higgs boson's Breit-Wigner propagator, respectively. The diphoton-invariant-mass distribution for the real-part interference is odd around the Higgs mass. It contributes negligibly to the experimentally observed cross section, which is integrated over the narrow line shape. The imaginary part interferes constructively or destructively with the signal distribution at the Higgs mass. For a light SM Higgs boson, the imaginary part vanishes at leading order in the zero quark mass limit [3]. The dominant contribution comes from the two-loop $gg \to \gamma\gamma$ amplitude and gives only a few percent suppression of the rate [4]. However, the real-part interference is affected by finite detector resolution, which smears the diphoton-invariant-mass distribution and causes a sizable shift in the apparent Higgs mass peak, as pointed out in Ref. [5] and further studied in Refs. [6,7].

In this Letter, we calculate the dominant next-to-leading-order (NLO) QCD corrections to the interference and study the dependence of the mass shift on the acceptance cuts. We further argue that the interference effect, especially the mass shift, can be used to bound experimentally, or possibly even measure, the Higgs width fairly directly, for widths well below the experimental mass resolution at the LHC. Such a measurement would complement even more direct measurements of the Higgs width at future colliders such as the ILC [8,9] or a muon collider [10,11] but might be accomplished much earlier.

Indirect bounds on the Higgs width at the LHC have also been given based on global analyses of various Higgs decay channels [12–14]. However, in these analyses, it is impossible to decouple the Higgs width from the couplings without a further assumption, because the Higgs signal strength is always given by the product of squared couplings for Higgs production and for decay, divided by the Higgs total width Γ_H. Typically, the further assumption is that the Higgs coupling to electroweak vector bosons does not exceed the SM value. For example, a recent CMS Collaboration analysis making this assumption obtained a 95% confidence level upper limit on the beyond-SM width of the Higgs boson of $0.64\Gamma_H$, corresponding to $\Gamma_H/\Gamma_H^{\rm SM} < 2.8$ [14]. Also, a Higgs width dominated by invisible modes can be ruled out by a direct search [15]. We demonstrate here that the interference effect, because of its different dependence on the Higgs width, allows Γ_H to be constrained independently of assumptions about couplings or new decay modes.

Theoretical description.—The NLO QCD formulas for Higgs production via gluon fusion are well known [16].

The SM continuum background for gluon fusion into two photons is also known at NLO [17]. [As a component of the inclusive diphoton background $pp \to \gamma\gamma X$, the process $gg \to \gamma\gamma$ technically begins at next-to-next-to-leading order (NNLO), but it is greatly enhanced by the large gluon parton distribution function (PDF) at small x.] Here, we present the dominant NLO corrections to the interference between the Higgs signal and background in QCD.

Figure 1 shows, first, the leading-order (LO) contribution to the interference [denoted by LO (gg)] of the resonant amplitude $gg \to H \to \gamma\gamma$ with the one-loop continuum $gg \to \gamma\gamma$ amplitude mediated by the five light quark flavors. We also include the tree-level process $qg \to \gamma\gamma q$, whose interference with $qg \to Hq \to \gamma\gamma q$ [denoted by LO (qg)] is at the same order in α_s as the leading $gg \to H \to \gamma\gamma$ interference, although suppressed by the smaller quark PDF. It was already considered in Refs. [6,7]. The contribution from $q\bar{q} \to Hg \to \gamma\gamma g$ is numerically tiny [6,7], and we will neglect it.

Finally, Fig. 1 depicts the three types of continuum amplitudes mediated by light quark loops that we include in the dominant NLO corrections [denoted by NLO (gg)]: the real radiation processes, $gg \to \gamma\gamma g$ and $qg \to \gamma\gamma q$ at one loop, and the virtual two-loop $gg \to \gamma\gamma$ process. All these amplitudes are adapted from Refs. [18–20]. The soft and collinear divergences in the real radiation process are handled by dipole subtraction [21,22]. Although the contribution from $qg \to \gamma\gamma q$ via a light quark loop is not the complete contribution to this amplitude, it forms a gauge-invariant subset and it is enhanced by a sum over quark flavors, so that it gives a significant contribution to the interference at finite Higgs transverse momentum.

In order to parametrize possible deviations from the SM in the coupling of the Higgs boson to the massless vector boson pairs gg and $\gamma\gamma$, we adopt the notation of Ref. [23] for the effective Lagrangian

$$\mathcal{L} = -\left[\frac{\alpha_s}{8\pi} c_g b_g G_{a,\mu\nu} G_a^{\mu\nu} + \frac{\alpha}{8\pi} c_\gamma b_\gamma F_{\mu\nu} F^{\mu\nu}\right]\frac{h}{v}, \quad (1)$$

where $b_{g,\gamma}$ are defined to absorb all SM contributions, and $c_{g,\gamma}$ differ from 1 in the case of new physics. We divide the line shape for the Higgs boson into a pure signal term and an interference correction, written schematically in the narrow-width approximation as

$$\frac{d\sigma^{\rm sig}}{dM_{\gamma\gamma}} = \frac{S}{(M_{\gamma\gamma}^2 - m_H^2)^2 + m_H^2\Gamma_H^2}, \quad (2)$$

$$\frac{d\sigma^{\rm int}}{dM_{\gamma\gamma}} = \frac{(M_{\gamma\gamma}^2 - m_H^2)R + m_H\Gamma_H I}{(M_{\gamma\gamma}^2 - m_H^2)^2 + m_H^2\Gamma_H^2}. \quad (3)$$

The signal factor S is proportional to $c_g^2 c_\gamma^2$, while the real and imaginary parts of the interference terms R and I are proportional to $c_g c_\gamma$. We take the resonance mass to be $m_H = 125$ GeV and the SM width to be $\Gamma_H^{\rm SM} = 4$ MeV [24]. In the narrow-width approximation, the integral of the cross section over the resonance is given by $\pi S/(2m_H^2\Gamma_H)$ and $\pi I/(2m_H)$ for signal and interference, respectively. Note that R has a different dependence on the Higgs width and couplings than does the integrated signal, i.e., $c_g c_\gamma$ versus $c_g^2 c_\gamma^2/\Gamma_H$. Hence, any effect due to R could be used to constrain Γ_H independently of the Higgs couplings.

The theoretical line shapes (2) and (3) are very narrow and strongly broadened by the experimental resolution. The main effect of the real term R after this broadening is to shift the apparent mass slightly [5]. Following Ref. [5], we model the experimental resolution by a Gaussian distribution. Although a definitive study of the apparent mass shift has to be performed by the experimental collaborations, using a complete description of the resolution and the background model, we estimate it as follows: For the distribution in the diphoton invariant mass M, the likelihood of obtaining N events with $M = M_1, M_2, \ldots, M_N$ is

$$L = \frac{\mathcal{L}^N}{N!} e^{-\tilde{N}} \prod_{i=1}^{N} \frac{d\tilde{\sigma}}{dM}\bigg|_{M=M_i}, \quad (4)$$

where $\mathcal{L}$ is the integrated luminosity. Variables with tildes denote the prediction of the "experimental model," a pure Gaussian with a variable mass parameter $\tilde{m}_H$. For the true distribution, obtained by convoluting the sum of Eqs. (2) and (3) with a Gaussian of the same width $\sigma = 1.7$ GeV, we use variables without tildes.

To fit for the shifted mass, we minimize the test statistic $t = -2\ln L$ with respect to $\tilde{m}_H$. We derived the following equation determining the mass shift $\Delta m_H \equiv \tilde{m}_H - m_H$:

$$0 = \delta\langle t\rangle \propto \int dM \frac{\frac{d\tilde{\sigma}}{dM} - \frac{d\sigma}{dM}}{\frac{d\tilde{\sigma}}{dM}} \delta\frac{d\tilde{\sigma}}{dM} \approx \int dM \frac{\frac{d\tilde{\sigma}}{dM} - \frac{d\sigma}{dM}}{\frac{d\sigma}{dM}} \delta\frac{d\tilde{\sigma}}{dM}$$
$$= \delta\left[\int dM \frac{(\frac{d\tilde{\sigma}}{dM} - \frac{d\sigma}{dM})^2}{2\frac{d\sigma}{dM}}\right], \quad (5)$$

where $\delta \equiv \delta/\delta\tilde{m}_H$. Because $d\sigma/dM$ in the denominator should include the large continuum background, which is

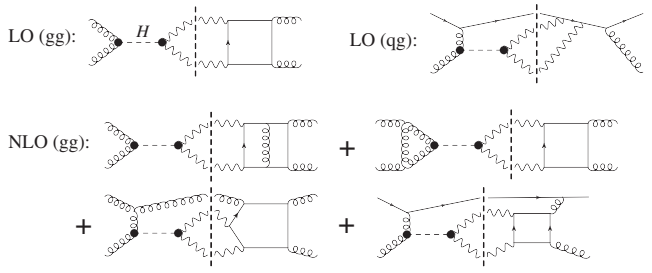

FIG. 1. Representative diagrams for interference between the Higgs resonance and the continuum in the diphoton channel. The dashed vertical lines separate the resonant amplitudes from the continuum ones.

roughly constant throughout the range of consideration, Eq. (5) reduces to a simple least-squares fit. The mass shift obtained from this fit is stable once we include invariant masses ranging out to three times the Gaussian width.

The top panel of Fig. 2 shows the Gaussian-smeared diphoton-invariant-mass distribution for the pure signal at both LO and NLO in QCD. We use the MSTW2008 NLO PDF set and α_s [25] throughout, and set $\alpha = 1/137$. Standard acceptance cuts are applied to the photon transverse momenta $p_{T,\gamma}^{\text{hard/soft}} > 40/30$ GeV and rapidities $|\eta_\gamma| < 2.5$. In addition, events are discarded when a jet with $p_{T,j} > 3$ GeV is within $\Delta R_{\gamma j} < 0.4$ of a photon. A jet veto is simulated by throwing away events with $p_{T,j} > 20$ GeV and $\eta_j < 3$. The scale uncertainty bands are obtained by varying $m_H/2 < \mu_F, \mu_R < 2m_H$ independently. Note that the NLO (gg) channel includes the contribution from the qg channel where the quark splits to a gluon; this reduces dependence on the factorization scale μ_F. As a result, the scale uncertainty bands mostly come from varying the renormalization scale μ_R.

The bottom panel of Fig. 2 shows the corresponding Gaussian-smeared interference contributions. The contribution involving the SM tree amplitude for $qg \to \gamma\gamma q$ is denoted by LO (qg). The destructive interference from the imaginary part I in Eq. (3) shows up at two-loop order in the gluon channel in the zero mass limit of light quarks [4].

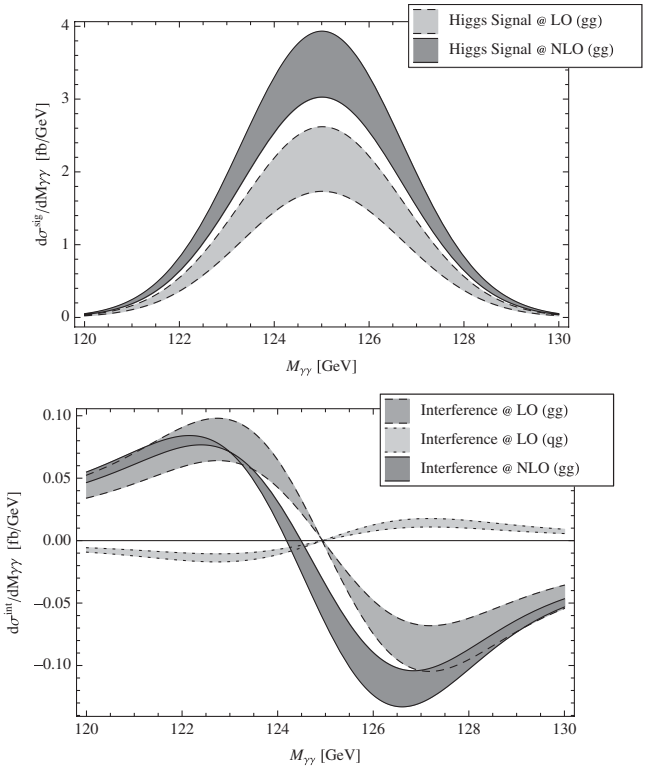

FIG. 2. Diphoton-invariant-mass $M_{\gamma\gamma}$ distribution for pure signal (top panel) and the interference term (bottom panel) after Gaussian smearing.

It produces the offset of the NLO (gg) curve from zero at $M_{\gamma\gamma} = 125$ GeV.

Mass shift and width dependence.—In Fig. 3, we plot the apparent Higgs boson mass shift versus the jet veto p_T cut. The mass shift for inclusive production (large $p_{T,\text{veto}}$) is around 70 MeV at NLO, significantly smaller than the LO prediction of 120 MeV. The reduction is mainly due to the large NLO QCD Higgs production K factor. The K factor for the SM continuum background is also sizable due to the same gluon incoming states. But, the Higgs signal is enhanced additionally by the virtual correction to the top quark loop, which is missing in the continuum background [17]. The K factor of the interference is between that of the signal and that of the background. This is reasonable but not inevitable, given that only a restricted set of helicity configurations enters the interference. For moderate jet veto cuts, the mass shift depends very weakly on p_T due to the smallness of the real radiation contribution. The extra interference with quark-gluon scattering at tree level reduces the mass shift a bit more, as shown in the curve labeled NLO (gg) + LO (qg) in Fig. 3. At small veto p_T, the results become unreliable: large logarithms spoil the convergence of perturbation theory, and resummation is required, which is beyond the scope of this Letter.

In Fig. 4, we remove the jet veto cut and study how the mass shift depends on a lower cut on the Higgs transverse momentum, $p_T > p_{T,H}$. This strong dependence could potentially be observed experimentally, completely within the $\gamma\gamma$ channel, without having to compare against a mass measurement using the only other high-precision channel, ZZ^*. (The mass shift for ZZ^* is much smaller than for $\gamma\gamma$, as can be inferred from Fig. 17 of Ref. [26], because $H \to ZZ^*$ is a tree-level decay, while the continuum background $gg \to ZZ^*$ arises at one loop, the same order as $gg \to \gamma\gamma$.) Using only $\gamma\gamma$ events might lead to reduced experimental systematics associated with the absolute photon energy scale. The $p_{T,H}$ dependence of the mass shift was first studied in Ref. [7]. The dotted dark gray band includes, in addition, the continuum process $qg \to \gamma\gamma q$ at one loop

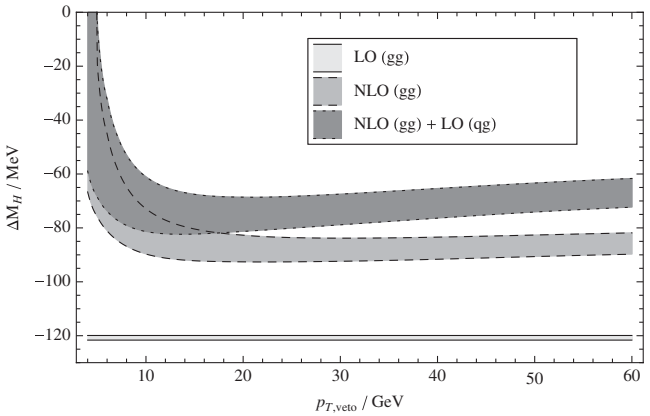

FIG. 3. Apparent mass shift for the SM Higgs boson versus jet veto p_T.

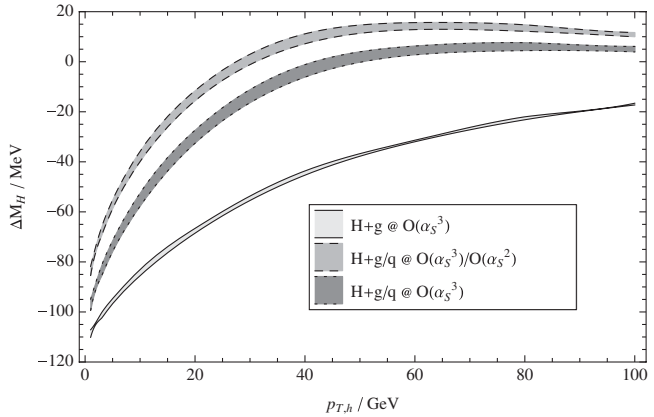

FIG. 4. Apparent mass shift for the SM Higgs boson versus the lower cut on the Higgs transverse momentum, $p_T > p_{T,H}$.

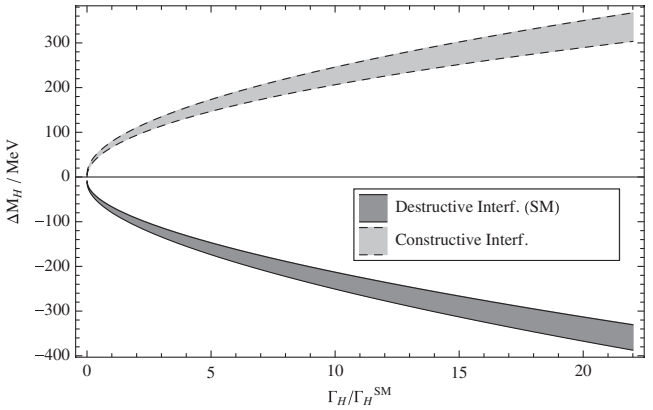

FIG. 5. Higgs mass shift as a function of the Higgs width. The coupling $c_{g\gamma}$ has been adjusted to maintain a constant signal strength, in this case $\mu_{\gamma\gamma} = 1$.

via a light quark loop, a part of the full $O(\alpha_s^3)$ correction. This new contribution partially cancels against the tree-level qg channel, leading to a larger negative Higgs mass shift. The scale variation of the mass shift at finite $p_{T,H}$ is very small because it is essentially a LO analysis; the scale variation largely cancels in the ratio between interference and signal that enters the mass shift.

Because of large logarithms, the small $p_{T,H}$ portion of Fig. 4 is less reliable than the large $p_{T,H}$ portion. In using the $p_{T,H}$ dependence of the mass shift to constrain the Higgs width, the theoretical accuracy will benefit from using a wide first bin in p_T. One could take the difference between apparent Higgs masses for $\gamma\gamma$ events in two bins, those having p_T above and below, say, 40 GeV.

Finally, we allow the Higgs width to differ from the SM prediction. The Higgs couplings to gluons, photons, and other observed final states should then change accordingly, in order to maintain roughly SM signal yields, as is in reasonable agreement with current LHC measurements. In particular, for the product $c_g c_\gamma = c_{g\gamma}$ entering the dominant gluon fusion contribution to the $\gamma\gamma$ yield, we solve the following equation:

$$\frac{c_{g\gamma}^2 S}{m_H \Gamma_H} + c_{g\gamma} I = \left(\frac{S}{m_H \Gamma_H^{\rm SM}} + I\right)\mu_{\gamma\gamma}, \tag{6}$$

where $\mu_{\gamma\gamma}$ denotes the ratio of the experimental signal strength in $gg \to H \to \gamma\gamma$ to the SM prediction ($\sigma/\sigma^{\rm SM}$). For Higgs widths much less than 1.7 GeV, the mass shift is directly proportional to $c_{g\gamma}/\mu_{\gamma\gamma}$. On the right-hand side of Eq. (6), the two-loop imaginary interference term I is negligible; the fractional destructive interference in the SM is $m_H \Gamma_H^{\rm SM} I/S \approx -1.6\%$. For $\Gamma_H \leq 100\Gamma_H^{\rm SM} = 400$ MeV, it is a good approximation to also neglect I on the left-hand side. Then, the solution for $c_{g\gamma}$ is simply $c_{g\gamma} = \sqrt{\mu_{\gamma\gamma}\Gamma_H/\Gamma_H^{\rm SM}}$. Figure 5 plots the mass shift, assuming $\mu_{\gamma\gamma} = 1$. It is indeed proportional to $\sqrt{\Gamma_H}$ for the widths shown in the figure, up to small corrections. If new physics somehow reverses the sign of the Higgs diphoton amplitude, the interference is constructive and the mass shift is positive.

In principle, one could apply the existing measurements of the Higgs mass in the ZZ^* and $\gamma\gamma$ channels in order to get a first limit on the Higgs width from this method. However, there are a few reasons why we do not do this here. First of all, the current ATLAS [27] and CMS [28] measurements are not very compatible,

$$\begin{aligned} m_H^{\gamma\gamma} - m_H^{ZZ} &= +2.3^{+0.6}_{-0.7} \pm 0.6 \text{ GeV (ATLAS)} \\ &= -0.4 \pm 0.7 \pm 0.6 \text{ GeV (CMS)}, \end{aligned} \tag{7}$$

where the first error is statistical and the second is systematic. Second, the experimental resolution differs from bin to bin and has non-Gaussian tails. Third, the precise background model can influence the apparent mass shift. What we can say is that taking $\Gamma_H = 200\Gamma_H^{\rm SM} = 800$ MeV and neglecting the latter factors would result in a mass shift of order 1 GeV, in the same range as Eq. (7). This is a considerably smaller width than the first direct bound from CMS, $\Gamma_H < 6.9$ GeV at 95% confidence level [29].

A measurement of Δm_H using two $p_{T,H}$ bins in the $\gamma\gamma$ channel is currently limited by statistics. At the high luminosity LHC, with 3 ab^{-1} of integrated luminosity at 14 TeV, the statistical error on Δm_H will drop to 50 MeV or less. The extrapolation of the systematic error is still somewhat uncertain but should result in a total error of 100 MeV or less [30]. From Fig. 5, this corresponds to a bound on the Higgs width at 95% C.L. that is within a factor of 15 of the SM value of 4 MeV.

Summary.—In this Letter, we have studied the interference of the SM Higgs boson with the LHC diphoton continuum background at NLO in QCD. The mass shift is largely stable for moderate jet veto p_T cuts. In addition, we provide a slightly more precise prediction for the mass shift at finite Higgs p_T by including the contribution from quark-gluon scattering via quark loops. The strong p_T dependence of the mass shift may allow its measurement

without reference to the ZZ^* channel. Furthermore, we consider a scenario in which new physics modifies the Higgs width without altering event rates in the diphoton channel. The mass shift increases rapidly with the Higgs width, which could lead to a more direct bound on the Higgs width than is presently available.

We are grateful to Florian Bernlochner, Glen Cowan, Daniel de Florian, Dag Gillberg, Louis Fayard, Tom Junk, Narei Lorenzo, Steve Martin, Jamie Saxon, and Reisaburo Tanaka for helpful comments. We thank Stefan Höche for useful discussions and help with the numerical implementation. This research was supported by the U.S. Department of Energy under Contract No. DE-AC02-76SF00515.

[1] S. Chatrchyan *et al.* (CMS Collaboration), Phys. Lett. B **716**, 30 (2012).
[2] G. Aad *et al.* (ATLAS Collaboration), Phys. Lett. B **716**, 1 (2012).
[3] D. A. Dicus and S. S. D. Willenbrock, Phys. Rev. D **37**, 1801 (1988).
[4] L. J. Dixon and M. S. Siu, Phys. Rev. Lett. **90**, 252001 (2003).
[5] S. P. Martin, Phys. Rev. D **86**, 073016 (2012).
[6] D. de Florian, N. Fidanza, R. J. Hernández-Pinto, J. Mazzitelli, Y. R. Habarnau, and G. F. R. Sborlini, Eur. Phys. J. C **73**, 2387 (2013).
[7] S. P. Martin, Phys. Rev. D **88**, 013004 (2013).
[8] F. Richard and P. Bambade, arXiv:hep-ph/0703173.
[9] M. E. Peskin, arXiv:1207.2516.
[10] T. Han and Z. Liu, Phys. Rev. D **87**, 033007 (2013).
[11] A. Conway and H. Wenzel, arXiv:1304.5270.
[12] B. A. Dobrescu and J. D. Lykken, J. High Energy Phys. 02 (2013) 073.
[13] A. Djouadi and G. Moreau, arXiv:1303.6591.
[14] S. Chatrchyan *et al.* (CMS Collaboration), CMS Report No. CMS PAS HIG-13-005, 2013 (unpublished).
[15] G. Aad *et al.* (ATLAS Collaboration), ATLAS Report No. ATLAS-CONF-2013-011, 2013.
[16] A. Djouadi, M. Spira, and P. M. Zerwas, Phys. Lett. B **264**, 440 (1991); S. Dawson, Nucl. Phys. **B359**, 283 (1991); D. Graudenz, M. Spira, and P. M. Zerwas, Phys. Rev. Lett. **70**, 1372 (1993); M. Spira, A. Djouadi, D. Graudenz, and P. M. Zerwas, Nucl. Phys. **B453**, 17 (1995).
[17] Z. Bern, L. J. Dixon, and C. Schmidt, Phys. Rev. D **66**, 074018 (2002).
[18] Z. Bern, L. J. Dixon, and D. A. Kosower, Phys. Rev. Lett. **70**, 2677 (1993).
[19] Z. Bern, L. J. Dixon, and D. A. Kosower, Nucl. Phys. **B437**, 259 (1995).
[20] Z. Bern, A. De Freitas, and L. J. Dixon, J. High Energy Phys. 09 (2001) 037.
[21] S. Catani and M. H. Seymour, Nucl. Phys. **B485**, 291 (1997); **B510**, 503(E) (1998).
[22] T. Gleisberg and F. Krauss, Eur. Phys. J. C **53**, 501 (2008).
[23] J. Ellis and T. You, J. High Energy Phys. 06 (2013) 103.
[24] A. Djouadi, J. Kalinowski, and M. Spira, Comput. Phys. Commun. **108**, 56 (1998).
[25] A. D. Martin, W. J. Stirling, R. S. Thorne, and G. Watt, Eur. Phys. J. C **63**, 189 (2009).
[26] N. Kauer and G. Passarino, J. High Energy Phys. 08 (2012) 116.
[27] G. Aad *et al.* (ATLAS Collaboration), arXiv:1307.1427.
[28] S. Chatrchyan *et al.* (CMS Collaboration), CMS Report No. CMS-PAS-HIG-13-001, 2013; CMS Report No. CMS-PAS-HIG-13-002, 2013.
[29] S. Chatrchyan *et al.* (CMS Collaboration), CMS Report No. CMS-PAS-HIG-13-016, 2013.
[30] F. Bernlochner, D. Gillberg, N. Lorenzo, and J. Saxon (private communication).